catalysts

MDPI

Article

Influences of MgO(001) and TiO_2(101) Supports on the Structures and Properties of Au Nanoclusters

Jinhua Gao [1,2,†], Yuehong Ren [1,2,†], Qingzhen Han [1,*], Hao Wen [1] and Zhaotan Jiang [2,*]

[1] State Key Laboratory of Multiphase Complex Systems, Research Department for Environmental Technology and Engineering, Institute of Process Engineering, Chinese Academy of Sciences, Beijing 100190, China; gaojinhua5@xdf.cn (J.G.); yhrenbitipe@163.com (Y.R.); hwen@ipe.ac.cn (H.W.)

[2] School of Physics, Beijing Institute of Technology, Beijing 100081, China

* Correspondence: qzhan@ipe.ac.cn (Q.H.); jiangzhaotan@hotmail.com (Z.J.); Tel.: +86-10-8261-2330 (Q.H.)

† These authors contributed equally to this work.

Received: 18 November 2019; Accepted: 18 December 2019; Published: 21 December 2019

Abstract: Due to the unique structures, photoelectric properties, good catalytic activity, and broad potential applications, gold nanoclusters (Au_n) received extensive attention in catalysis, bioengineering, environmental engineering, and so on. In the present work, the structures and properties of Au_n adsorbed on the MgO(001) and TiO_2(101) surfaces were investigated by density functional theory. The results showed that the catalytic properties of Au_n will be enhanced when Au_n is adsorbed on certain supports. Because the difference of the outer electronic structure of metals in supports, the direction of the charge transfer was different, thus inducing the different charge distribution on Au_n. When Au_n was adsorbed on MgO(001) [TiO_2(101)] surface, Au_n will have negative [positive] charges and thus higher catalytic activity in oxidation [reduction] reaction. The variation of surface charges caused by the support makes Au_n possess different catalytic activity in different systems. Moreover, the electronic structure of the support will make an obvious influence on the s and d density of states of Au_n, which should be the intrinsic reason that induces the variations of its structure and properties. These results should be an important theoretical reference for designing Au_n as the photocatalyst applied to the different oxidation and reduction reactions.

Keywords: Au nanoclusters; adsorption; binding energy; electronic structure; catalytic activity

1. Introduction

The research on gold nanoclusters (Au_n) started to attract extensive attention when Haruta et al. [1] found that Au_n on TiO_2 have a good catalytic activity in CO low-temperature oxidation reaction. Further deep explorations of Au_n uncovered that Au_n not only exhibited a variety of physical and chemical features [2–4], but also had broad applications in many fields, such as catalysis, biological engineering, nanotechnology, and so on [5–10]. More importantly, the study on the Au_n is still the research focus even now.

Among the factors of determining the Au_n physical and chemical features, the structures of Au_n are found to play a crucial role. In the theoretical aspect, Häkkinen et al. [11] and Min et al. [12] found that the neutral Au_n will prefer the two-dimensional structures when the atom number n is less than 13. Research of the Au_n ($2 \leq n \leq 9$) structures carried out by Mao et al. [13] indicates that with the increasing of n the average binding energy per atom will increase gradually, and an odd-even oscillation will appear in the Fermi energy, the electron affinity energy, and the ionization potential energy. Moreover, Bulusu et al. [14] investigated the Au_n with n = 15∼19 and revealed that the Au_n structure will be transformed to the hollow structure at n = 17 and the pyramid structure at n = 19. Also, Fa et al. [15] found that Au_n will be the two-dimensional planar structures in the case of $n \leq 12$

and the transition from the planar to the three-dimensional structures will take place at n = 13∼15. Zhao et al. [16] found that the ground-state geometry of Au_n (n = 19∼22) is tetrahedron, and Au_{24} is a tube-like structure. All the researches indicate that the Au_n structures are closely dependent on the Au_n size.

On the other hand, great attention has also been paid to the study of the Au_n adsorbed on metal oxide surface, especially MgO and TiO_2. Yoon et al. [17] found that Au_8 on the MgO surface will show a good catalytic activity in the CO oxidation reaction because the charges are transferred from MgO surface to Au_n. Liu et al. [18] reported that the structure of Au_n will be a three-dimensional structure at n = 7 in the study of Au_n (n = 1∼8) vertically adsorbed on the surface of MgO(001). Roldan et al. [19] studied the adsorption activity of the O_2 activation on Au_5/MgO, and Stamatakis et al. [20] investigated the CO oxidation on Au_n/MgO. Both these two works demonstrate that the charge transfer occurring between the clusters and the O_2 promotes the adsorption of oxygen. Meanwhile, many researches on Au_n/TiO_2 have also begun. Kim et al. [21] found that the charge transfer between support materials and the Au_n will increase the catalytic activity of the clusters. The study of the stability of Au_n on anatase TiO_2(110) surface carried out by Pabisiak et al. [22] showed that the finite linear Au_n clusters will be formed on the highly defected surface. Asakura [23] found that Au anion is very important for the stability of Au_n adsorbed on TiO_2(110) surface. At the same time, Li et al. [24] explored the influence of Au_n/TiO_2 on CO oxidation and showed that the reaction rate is dependent on the size and shape of the Au_n. Recently, Cao et al. [25] found that the charge transfer between Au_n and TiO_2(110) depends on the number of oxygen free radicals and the size of Au_n.

All the researches indicate that the chemical and physical properties of Au_n are closely related to its structure, its size, and the surfaces of the supports. Although many researches of Au_n adsorbed on metal oxide surfaces have been done, the intrinsic mechanism and the meso-scale control mechanism combining the macroscopic properties with the microscopic electronic structures are still not quite clear. So a further systematic research of Au_n on MgO(001) and anatase TiO_2(101) surfaces is required. In this paper, Au_n, Au_n/MgO(001), and Au_n/TiO_2(101) will be studied by using the density functional theory (DFT) [26,27]. The transition of the geometric structure, the variations of the average bond lengths and the partial density of states (PDOS), and the charge transfer will be discussed. Furthermore, the reasons why these variations appear and the possible intrinsic mechanisms will be analyzed.

2. Results and Discussion

2.1. Geometric Structures of Au_n

To find the steadiest adsorption site of Au atom on the supports, four types of initial structures (Figure 1) will be considered including O atom top, Mg atom top, Mg-O bridge, and Mg-O hole. After optimization, Au atoms initially adsorbed on Mg-O bridge or Mg-O hole will be moved to the site of O atom top. Also, the adsorption energy of the Au atom on the top site of O atoms is found to be less than that on Mg atoms. Therefore, we can draw a conclusion that the steadiest adsorption site should be the top site of O atom, which is in accordance with the results reported in the literature [28–30]. For each Au_n with a certain atom number n, its steadiest configuration on the supports will be determined by comparing lots of optimized structures obtained from different initial configurations.

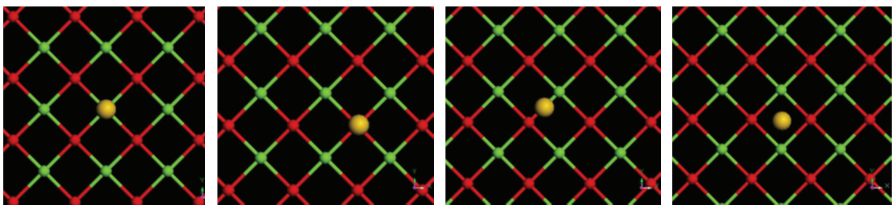

Figure 1. Typical initial structures of Au/MgO.

Figures 2–4 show the optimized structures of Au_n in vacuum, Au_n on MgO(001) surface, and Au_n on TiO_2(101) surface, respectively. By comparing the corresponding stable structures of Au_n, Au_n/MgO(001) and Au_n/TiO_2(101), we can see that Au_n structures are distorted obviously when they are adsorbed on the MgO(001) and TiO_2(101) surfaces. In the case of Au_n/MgO(001), the bond length of Au_2 on MgO(001) almost does not change and Au_2 is askew adsorbed on the surface, as shown in Figure 3. Au_3 on MgO(001), retaining a planar structure similar to that in vacuum, is adsorbed with the plane perpendicular to MgO(001) surface. In the corresponding side view, the middle Au atom is far away from the surface of MgO(001), but still on the top of oxygen atoms, which is in accordance with the references [28,29]. The structures of Au_n (n = 4∼13) on MgO(001) surface show partial distortion. In the top view, they seem to maintain the same basic structures as in vacuum, while in the side view obvious distortions can be observed. Au atoms located on the sites of the top and bridge of O atom are moved far away from the MgO(001) surface, but Au atoms on other sites are moved close to the MgO(001) surface, which makes the flat structures distort. Au_{14} shows a three dimensional flat cage structure in vacuum, but distorts seriously when it is adsorbed on MgO(001) with the atoms near MgO surface almost in one plane. For another three-dimensional flat cage structure, Au_{15} will change little when it is adsorbed on MgO(001). On TiO_2(101) surface, Au_3 structure does not distort obviously, and the bond length is only slightly stretched. For other Au_n, roughly speaking, they show similar distortion with its bond lengths longer than those in vacuum, and with these variations less than those on MgO(001) surface. The changes of the structures of Au_n on MgO(001) and TiO_2(101) surfaces show that the adsorption properties of Au_n ($n \lesssim 4$) are different from Au_n ($n \gtrsim 5$). Moreover, these results show that when Au_n are adsorbed on metal oxide surface, some atoms in the Au_n plane will move up and others will move down relative to the original Au_n plane, making the bonds stretched and the flat structure become a quasi-flat structure, which will be beneficial for improving the catalytic activity of Au_n.

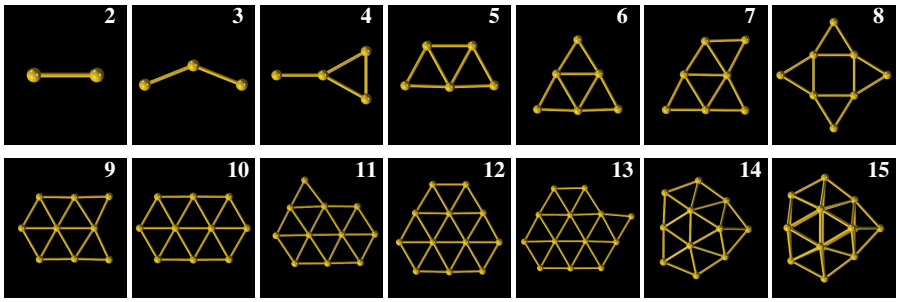

Figure 2. Structures of Au_n with n = 2, 3, · · · · · , 15 in vacuum.

Furthermore, we analyze the adsorption energy E_a, the binding energy E_b, the internal binding energy E_c and the average bond length for Au_n on MgO(001) and TiO_2(101) with different n in Figure 5. In Figure 5a, it can be found that the adsorption energy of some Au_n is very large, such as 1.51 eV (0.78 eV) for Au (Au_2) on the MgO(001), and 0.62 eV for Au_2 on the TiO_2(101), possibly implying that the adsorption between Au_n ($n \lesssim 4$) and supports should be the chemisorption, while other Au_n ($n \gtrsim 5$) may be adsorption. Meanwhile, the average adsorption energy of Au_n tends to decrease with the increase of the number n of Au_n on MgO(001) surface, and approaches zero. This means that Au_n in enough large size is difficult to be adsorbed on metal oxide surface. Except Au_5/TiO_2(101), all the adsorption energy values of other Au_n on TiO_2(101) are smaller than the counterparts of Au_n on MgO(001). This demonstrates that Au_n on Mg(001) surface may possess stronger stability. For Au_n on TiO_2(101) surface, Au_5 is almost the steadiest adsorption structure except the chemisorption of Au_2. Figure 5b gives the variations of E_b of Au_n adsorbed on MgO(001) and TiO_2(101). Either on MgO(001) or TiO_2(101) surface, the E_b increases with the increase of Au atom number n. The E_b of Au_n on MgO(001) becomes nearly invariant when $n \gtrsim 6$, while on TiO_2 surface, it will become invariant when $n \gtrsim 7$. This indicates that Au_n of larger size is steadier than the smaller one, and the

smaller Au_n cluster may incline to merge to a larger one. In Figure 5c, the E_c of Au_n also increases with the atom number n of Au_n. The corresponding E_c will be reduced when Au_n is adsorbed on metal oxide surface, especially on TiO_2(101) surface. The interaction between TiO_2 and Au_n is more beneficial for polymerizing. By comparing the values of E_a with E_c for Au_n on the same metal support in the same size in Figure 5a,c, we can see that the E_c within cluster ($n \geq 5$) is always larger than the E_a. This demonstrates that the interaction of Au-Au in clusters is stronger than that of Au-O and Au-Mg, likewise for Au-O and Au-Ti, further indicating that either adsorbed on TiO_2(101) or MgO(001), Au atoms prefer to exist in the form of clusters. The bond length of Au_n corresponding to different n is given in Figure 5d. For clarity, the corresponding structure data before and after Au_n adsorption are also shown in Table 1. It can be found that all the adsorption-induced variations of the structure data for Au-Au, Mg-O, and Ti-O are in the range $-0.081 \backsim 0.081$ Å . For Au_n of the same atom number, except Au_2, all the average Au-Au bond lengths of Au_n adsorbed on metal oxide is longer than that in vacuum, indicating the activity will be improved. In addition, the variation of Au-Au bond length in Au_n/MgO(001) is larger than that in Au_n/TiO_2(101), meaning that the activity of Au_n on MgO(001) is higher, which agrees about the analysis of adsorption energy. As presented in references [31–33], the bond length variation in cluster is closely dependent on the competition between the cluster-support interaction and the intrinsic interaction within the cluster. Here, since E_c is greater than E_a for Au_n ($n \gtrsim 5$), the increase of the average Au-Au bond length is very tiny.

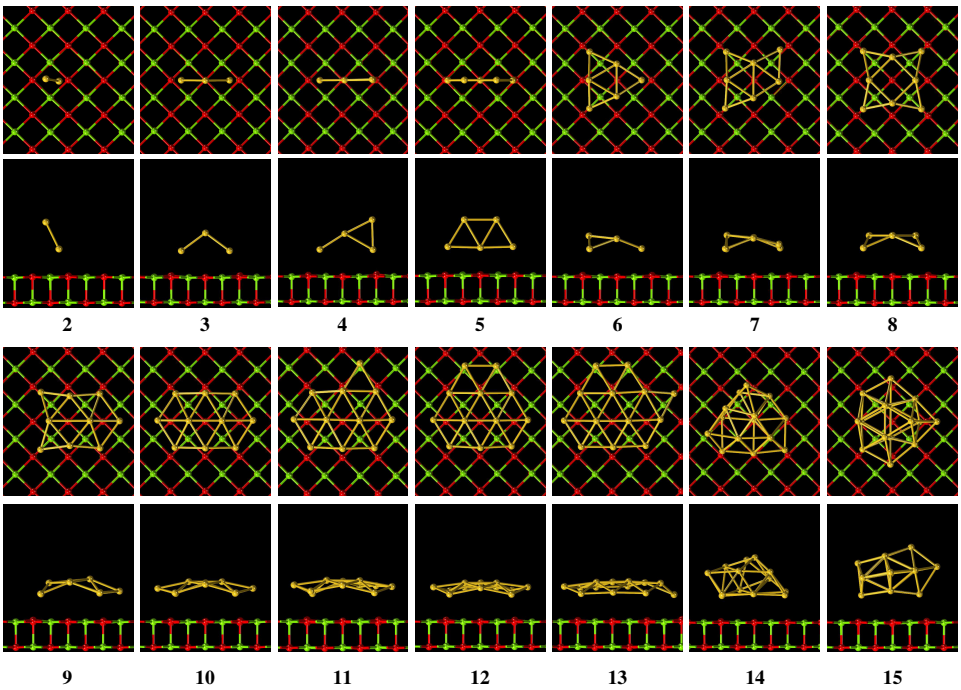

Figure 3. Top and side view of the Au_n/MgO(001) structures.

Table 1. Structure data of Au_n, Au_n/MgO(001), and Au_n/TiO_2(101).

	Au_n	Au_n/MgO(001)		Au_n/TiO_2(101)	
	Au-Au (Å)	**Mg-O (Å)**	**Au-Au (Å)**	**Ti-O (Å)**	**Au-Au (Å)**
0	–	2.101	–	2.035	–
2	2.558	2.173	2.557	2.110	2.549
3	2.589	2.192	2.631	2.077	2.618
4	2.656	2.187	2.691	2.082	2.667
5	2.717	2.169	2.741	2.019	2.698
6	2.714	2.198	2.740	2.067	2.718

Table 1. *Cont.*

	Au_n	Au_n/MgO(001)		Au_n/TiO_2(101)	
	Au-Au (Å)	Mg-O (Å)	Au-Au (Å)	Ti-O (Å)	Au-Au (Å)
7	2.723	2.210	2.731	2.071	2.729
8	2.700	2.198	2.720	2.043	2.725
9	2.738	2.199	2.750	2.054	2.744
10	2.743	2.175	2.768	2.038	2.745
11	2.743	2.213	2.766	2.039	2.757
12	2.746	2.187	2.767	2.048	2.772
13	2.747	2.186	2.769	2.048	2.764
14	2.807	2.177	2.832	2.041	2.848
15	2.822	2.157	2.831	2.047	2.851

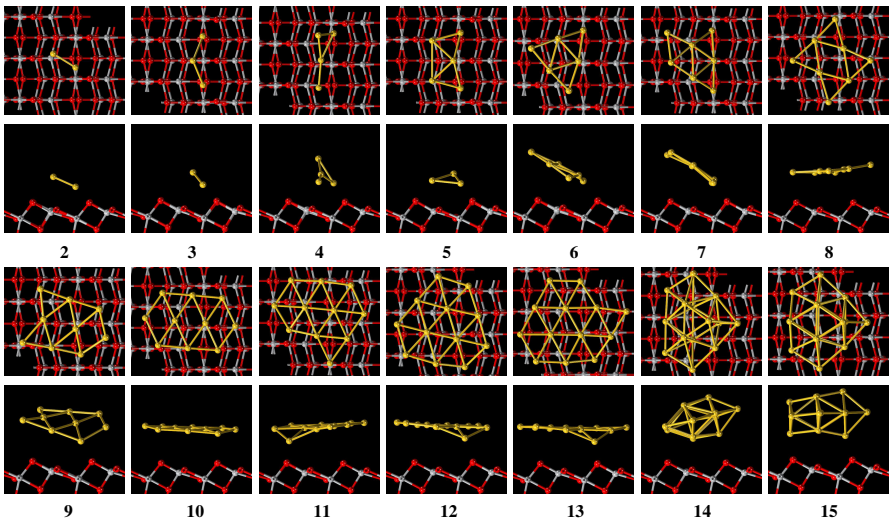

Figure 4. Top and side view of the Au_n/TiO_2(101) structures.

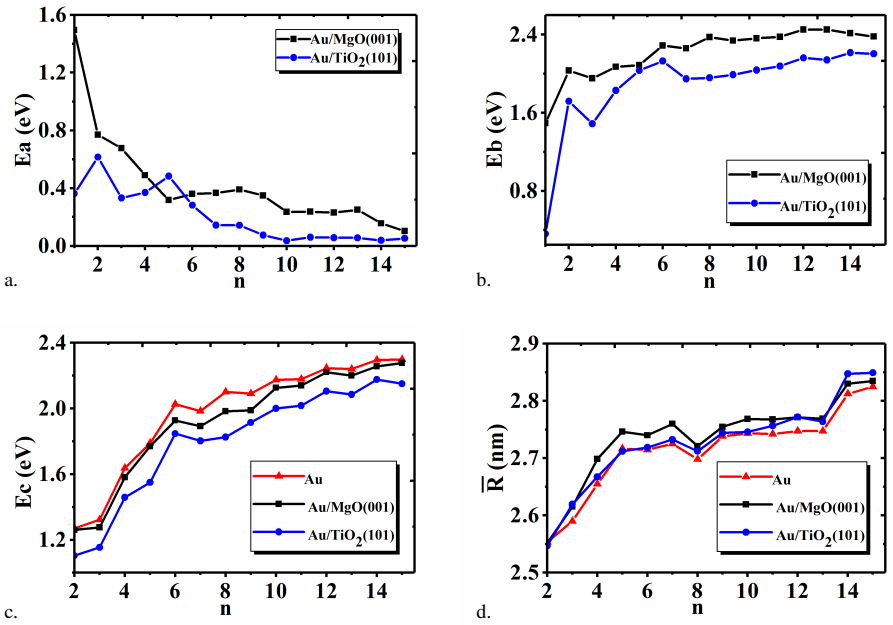

Figure 5. Average adsorption energy Ea (**a**), average binding energy Eb (**b**), internal binding energy Ec (**c**), and average Au-Au bond length $\overline{R}$ (**d**) of Au_n, Au_n/MgO(001), and Au_n/TiO_2(101) versus the atom number n.

2.2. PDOS

To study the effect of the adsorption-induced variation of the internal electronic structures of Au_n on the catalytic activity, we present all the related PDOS in Figure 6. First, we show the PDOS of O and Mg atoms in the surface of pure MgO(001) in Figure 6a. Clearly, it is the PDOS of p state of O atom that plays the dominant contribution. Therefore, we further only show the PDOS of p state of the O atom in the surface layer of the pure MgO(001), MgO(001) adsorbed with Au_6, and Mg(001) adsorbed with Au_8 in Figure 6b. Obviously, a whole shift of the PDOS toward the low energy direction will appear due to the adsorption of Au_6 or Au_8. This will cause the decrease of the corresponding PDOS value at Fermi energy, which also indicates that the adsorption of Au_6 or Au_8 will lead to the variation of the electron structure of the O atom in MgO(001) surface. In Figure 6c, we plot the PDOS of Au_2, Au_2/MgO(001), and Au_2/TiO_2(101). It can be found that in Au_2 the PDOS of s and d states of Au_2 will play the dominant contribution. Also, the peaks become broader in width and lower in height, and eventually three peaks incline to merge into a wider peak. Furthermore, we can see that the adsorption will push the three peaks below the Fermi energy to the low energy direction. In addition, the two peaks above the Fermi energy disappear for Au_2/TiO_2(101), and the two peaks will approach each other for Au_2/MgO(001). These imply that the different supports are able to induce the different variations of the PDOS of the s and d states in Au_n. Thus, the electronic structures of Au_2 on MgO(001) and TiO_2(101) surface will be changed due to adsorption. Eventually, this should be beneficial to improving the Au_n catalytic activity.

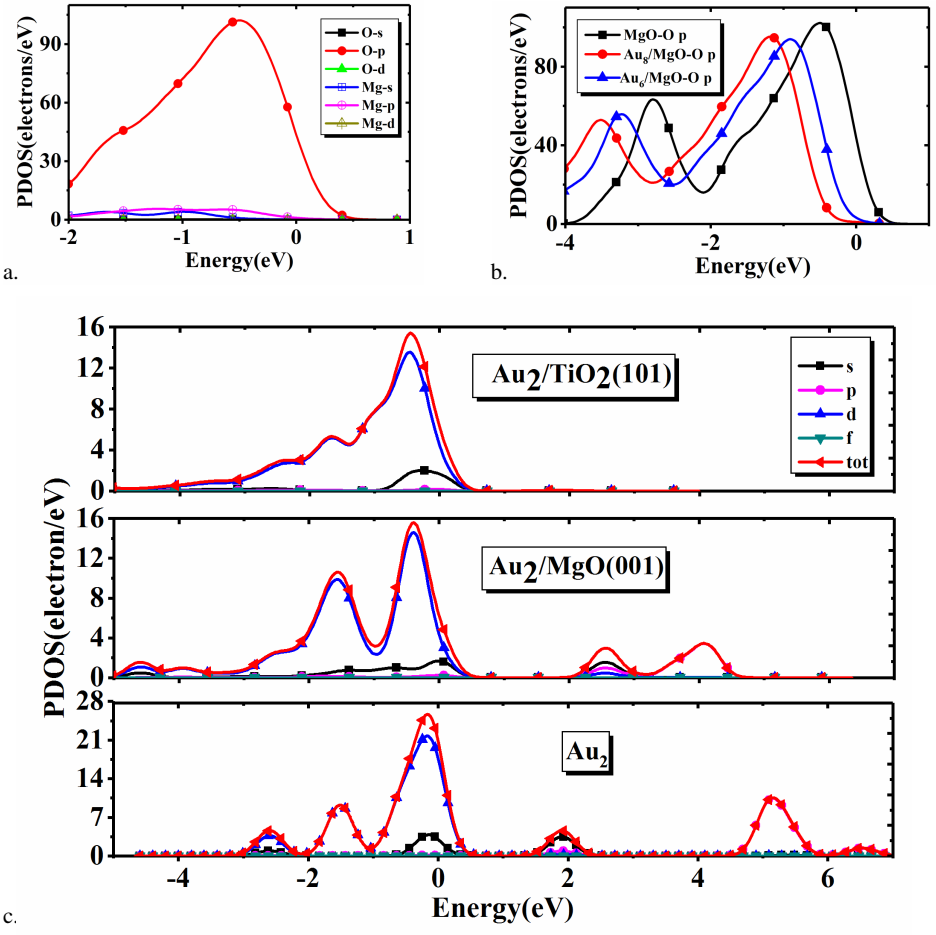

Figure 6. (**a**) PDOS of O and Mg atoms in MgO(001), (**b**) PDOS of p state of O atom in the surface layer of pure MgO(001), MgO(001) adsorbed with Au_6, and Au_8 clusters, respectively, and (**c**) PDOS of Au_2, Au_2/MgO(001) and Au_2/TiO_2(101).

2.3. Charge Transfer

As demonstrated in many works [34–36], charge transfer is a key factor in improving the catalytic activity of Au_n. Therefore, we intend to investigate the charge transfer occuring in $Au_n/MgO(001)$ and $Au_n/TiO_2(101)$. As examples, the electron density differences of $Au_8/MgO(001)$ and $Au_5/TiO_2(101)$ are shown in Figure 7a,b, respectively. Also, in Figure 8 we show the Mülliken charge distribution of Au_5, TiO_2, and $Au_5/TiO_2(101)$. Meanwhile, for clarity, the corresponding charge transfer data are listed in Table 2. In Figure 7a, the negative charges accumulate around atoms of Au_8, while the negative charges near the O and Mg atoms connected with Au_n atoms decrease. This demonstrates that the electrons transferring from Mg-O to Au atoms, makes Au_8 have negative charges. On the other hand, from the Mülliken charge distribution of $Au_8/MgO(001)$ (see Table 2), the same conclusion can be drawn. Obviously, the whole charges of each Au_n and the charges of every Au atom in Au_n are all negative when Au_n is adsorbed on MgO(001). This indicates that the negative charges transfer from MgO surface to Au_n, which is consistent with the studies of Roldan [19] and Stamatakis [20]. Different from the case of MgO(001) surface, charges will accumulate near O atom of the $TiO_2(101)$ which is close to Au atoms when Au_5 is adsorbed on $TiO_2(101)$, as shown in Figures 7b and 8, and Table 2. The charges of the two Au atoms directly connected to TiO_2 surface change from −0.06 to 0.06, and the charges of the central Au atom change from 0.09 to 0.03. Consequently, the whole charges of Au_5 change from 0.00 to 0.23. These phenomena suggest that the negative charges will transfer from Au atoms to TiO_2 surface, inducing that Au_n has positive charges. Therefore we conclude that the charge transfer direction in $Au_8/MgO(001)$ is different from that in $Au_5/TiO_2(101)$.

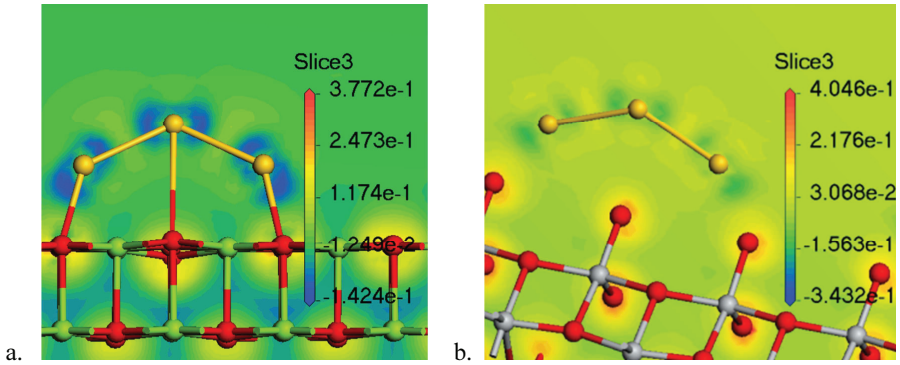

Figure 7. Electron density differences of $Au_8/MgO(001)$ (**a**) and $Au_5/TiO_2(101)$ (**b**).

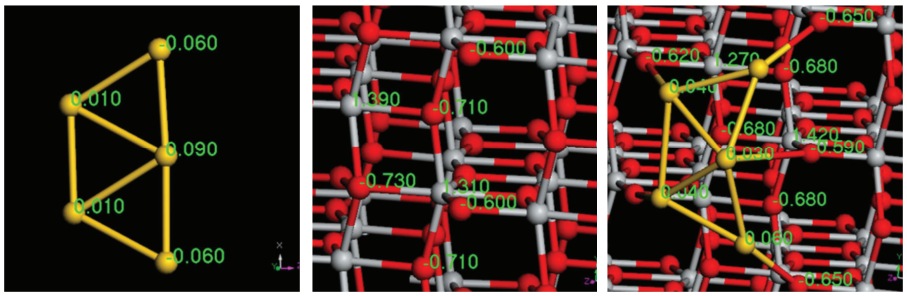

Figure 8. Mülliken charge distribution of Au_5, $TiO_2(101)$, and $Au_5/TiO_2(101)$.

To understand the direction of the electron transfer between Au_n and supports, we should resort to the outer electron structure of the metal as reported in reference [33]. The outer electron structure of Au, Mg, and Ti are $5d^{10}6s^1$, $3s^2$, and $3d^24s^2$, respectively. Obviously, Au has an almost filled 5d orbit and half-filled s orbit, and Mg has no d orbit, while Ti has unfilled 3d orbits, inducing that the charge can flow from Mg-O to Au or from Au to Ti-O. Fundamentally speaking, the different direction of charge flow is determined by the difference of the outer electron structure of the metal d orbit. Therefore, the negative charges flow from Mg-O in MgO(001) to Au and finally Au has

negative charges, which makes the Au_n possess high catalytic activity in oxidation reaction. However, the negative charges flow from Au to Ti-O in TiO_2(101) and finally Au has positive charges, which makes the Au_n possess high catalytic activity in reduction reaction. Therefore, catalytic activity of Au_n can be controlled by choosing suitable metal oxide supports.

Table 2. The Mulliken charge distribution of Au_n in different systems.

	Adsorption Site	Central Site	Total
Au_5	−0.06	0.09	0.00
Au_8	−0.08	0.08	0.00
Au_5/TiO_2(101)	0.06	0.03	0.23
Au_5/MgO(001)	−0.31	−0.13	−1.16
Au_8/MgO(001)	−0.36	−0.11	−1.88
Au_2/MgO(001)	−0.23	−0.21	−0.44
Au_3/MgO(001)	−0.30	−0.20	−0.80
Au_4/MgO(001)	−0.39	−0.18	−1.01
Au_6/MgO(001)	−0.35	−0.12	−1.36
Au_7/MgO(001)	−0.37	−0.11	−1.66

3. Materials and Methods

All calculations are performed by the plane-wave ultrasoft pseudo potential method based on DFT with the CASTEP [37] program of Material Studio package. The GGA-PBE [38,39] version of exchange-correlation energy function is applied, which was proved to be reasonable [40]. The cutoff energy for the plane wave basis set is 340 eV and the total energy convergence criterion for the self-consistent field (SCF) is 1.0×10^{-5} eV/atom. Based on the literature [41–46] and our experience, the MgO(001) and TiO_2(101) should be the absorption surfaces. Calculations of the two systems are performed for a two layer slab [41] with 6×6 surface periodicity and 3 Å [47,48] with 3×3 surface periodicity respectively, and both separated from their replicas by vacuum region of 15 Å width.

First of all, the stablest structures can be determined by optimizing Au_n structures in vacuum with the atom number ranging from 1 to 15. Then the chosen structures are adsorbed on MgO(001) and TiO_2(101) surfaces, respectively, which will be optimized further. Finally, the steadiest structures of the two systems can be determined according to the adsorption energy, the binding energy, and the average bond length. The adsorption energy per Au atom is calculated by the formula

$$E_a = (E_s + E_n - E_t)/n. \quad (1)$$

Here E_t stands for the total energy of the Au_n/sub system while E_s and E_n represent the energies of the isolated oxide substrate and the Au_n clusters, respectively. Therefore, a larger adsorption energy will indicate a stronger adsorption between cluster and support. The binding energy (per Au atom) of Au atom and oxide substrate is calculated via the formula

$$E_b = (E_s + nE_0 - E_t)/n, \quad (2)$$

where E_0 is the energy of an isolate Au atom calculated in a large cell. In addition, the internal binding energy E_c and the average bond length $\overline{R}$ of Au_n are calculated according to the following formulae:

$$E_c = E_b - E_a = E_0 - E_n/n, \quad (3)$$

$$\overline{R} = (1/m)\sum_i R_{ij}. \quad (4)$$

Here R_{ij} denotes the distance between Au atoms i and j in Au_n and m represents the number of bonds in Au_n.

Aiming at uncovering the intrinsic mechanism of the adsorption-induced influences on the properties of Au_n, our research was carried out in vacuum at 0 K and 1 atm.

4. Conclusions

The structures and properties of Au_n adsorbed on different metal oxide supports were studied by DFT. The following results are obtained: (1) The catalytic activity of Au_n becomes higher when they are adsorbed on metal oxide surface; (2) With the increase of Au atom number n, the binding energy increases while the adsorption energy between clusters and metal oxide decreases; (3) For the same size, the Au_n of $Au_n/MgO(001)$ has higher catalytic activity than that of $Au_n/TiO_2(101)$; (4) The direction of charge flow is determined by the outer electron structure of Au atom and metal atom of the oxide surface when Au_n is adsorbed on the oxide surface. In the system of $Au_n/MgO(001)$, charges flow from Mg-O to Au, indicating that Au_n has negative charges, which leads to high catalytic activity in oxidation reaction, while in the system of $Au_n/TiO_2(101)$, the direction of charge flow is reversed and Au_n has positive charges, leading to high catalytic activity in reduction reaction. This research may provide a theoretical reference for the design of the structures of Au_n catalyst, as well as the further study of its stability and catalytic properties.

Author Contributions: Conceptualization, H.W. and Z.J.; Data analysis, J.G.; Writing—original draft preparation, Q.H.; Writing—review and editing, Y.R. All authors have read and agreed to the published version of the manuscript.

Funding: This research was funded by the National Key Research and Development Program of China (No. 2017YFC0210304), the National Natural Science Foundation of China (Nos. 11774029, 11504374), and the CAS Informatization Program of the Thirteenth Five-Year Plan (No. XXH1350303-103).

Conflicts of Interest: The authors declare no conflict of interest.

References

1. Haruta, M.; Kobayashi, T.; Sano, H.; Yamada, N. Novel gold catalysts for the oxidation of carbon monoxide at a temperature far below 0 °C. *Chem. Lett.* **1987**, *16*, 405–408. [CrossRef]
2. Chang, C.M.; Chou, M.Y. Alternative Low-Symmetry Structure for 13 Atom Metal Clusters. *Phys. Rev. Lett.* **2004**, *93*, 133401. [CrossRef] [PubMed]
3. Wang, J.; Wang, G.; Zhao, J. Density-functional study of Au_n (n = 2–20) clusters: Lowest-energy structures and electronic properties. *Phys. Rev. B* **2002**, *66*, 035418. [CrossRef]
4. Fernandez, E.M.; Soler, J.M.; Balbás, L.C. Planar and cagelike structures of gold clusters: Density-functional pseudopotential calculations. *Phys. Rev. B* **2006**, *73*, 235433. [CrossRef]
5. Yang, Q.; Liu, J.; Chen, H.; Wang, X.; Huang, Q.; Shan, Z. Preparation of noble metallic nanoclusters and its application in biological detection. *Prog. Chem.* **2011**, *23*, 880–892.
6. Yan, F.; Liu, X.; Zhao, D.; Bao, W.; Xi, F. Application of Fluorescent Gold Nanoclusters for the Determination of Small Molecules. *Prog. Chem.* **2013**, *25*, 799–808.
7. Shang, L.; Dong, S.; Nienhaus, G.U. Ultra-small fluorescent metal nanoclusters: Synthesis and biological applications. *Nano Today* **2011**, *6*, 401–418. [CrossRef]
8. Li, Y.; Chen, Y.; House, S.D.; Zhao, S.; Wahab, Z.; Yang, J.C.; Jin, R. Interface Engineering of Gold Nanoclusters for CO Oxidation Catalysis. *ACS Appl. Mater. Interfaces* **2018**, *10*, 29425–29434. [CrossRef]
9. Moon, Y.K.; Jeong, S.Y.; Kang, Y.C.; Lee, J.H. Metal Oxide Gas Sensors with Au Nanocluster Catalytic Overlayer: Toward Tuning Gas Selectivity and Response Using a Novel Bilayer Sensor Design. *ACS Appl. Mater. Interfaces* **2019**, *11*, 32169–32177. [CrossRef]
10. Burgos, J.C.; Mejia, S.M.; Metha, G.F. Effect of Charge and Phosphine Ligands on the Electronic Structure of the Au_8 Cluster. *ACS Omega* **2019**, *4*, 9169–9180. [CrossRef]
11. Haekkinen, H.; Yoon, B.; Landman, U.; Li, X.; Zhai, H.J.; Wang, L.S. On the Electronic and Atomic Structures of Small Au_n(n = 4–14) Clusters: A Photoelectron Spectroscopy and Density Functional Study. *Chem. Inf.* **2003**, *107*, 6168–6175. [CrossRef]
12. Min, B.J.; Shin, W.C.; Park, J.I. Plane-wave Density Functional Theory Study of the Electronic and Structural Properties of Ionized and Neutral Small Gold Clusters. *New Phys. Sae Mulli* **2017**, *67*, 480–484. [CrossRef]

13. Mao, H.P.; Wang, H.Y.; Ni, Y.; Xu, G.L.; Ma, M.Z.; Zhu, Z.H.; Tang, Y.J. Geometry and electronic properties of Au_n(n = 2–9) clusters. *Acta Phys Sin.* **2004**, *53*, 1766–1771.
14. Bulusu, S.; Zeng, X.C. Structures and relative stability of neutral gold clusters: Au_n (n = 15–19). *J. Chem. Phys.* **2006**, *125*, 154303. [CrossRef]
15. Fa, W.; Luo, C.; Dong, J. Bulk-fragment and tube-like structures of Au_n (n = 2–26). *Phys. Rev. B* **2005**, *72*, 3182–3184. [CrossRef]
16. Zhao, H.Y.; Ning, H.; Wang, J.; Su, X.J.; Guo, X.G.; Liu, Y. Structural evolution of Au_n (n = 20–32) clusters: Lowest-lying structures and relativistic effects. *Phys. Lett. A* **2010**, *374*, 1033–1038. [CrossRef]
17. Yoon, B. Charging Effects on Bonding and Catalyzed Oxidation of CO on Au_8 Clusters on MgO. *Science* **2005**, *307*, 403–407. [CrossRef]
18. Liu, J.; Shunfang, L.I.; Haisheng, L.I. Study on First-Pinciples Calculations of Adsorption of Gold Clusters Au_n (n$\leq$ 8) on MgO(001) Surface. *Mater. Rev.* **2008**, *2*, 232–236.
19. Roldan, A.; Ricart, J.M.; Illas, F.; Pacchioni, G. O_2 Activation by Au_5 Clusters Stabilized on Clean and Electron-Rich MgO Stepped Surfaces. *J. Phys. Chem. C* **2010**, *114*, 16973–16978. [CrossRef]
20. Stamatakis, M.; Christiansen, M.A.; Vlachos, D.G.; Mpourmpakis, G. Multiscale Modeling Reveals Poisoning Mechanisms of MgO-Supported Au Clusters in CO Oxidation. *Nano Lett.* **2012**, *12*, 3621–3626. [CrossRef]
21. Kim, Y.D.; Fischer, M.; Gantefor, G. Origin of unusual catalytic activities of Au-based catalysts. *Chem. Phys. Lett.* **2003**, *377*, 170–176. [CrossRef]
22. Pabisiak, T.; Kiejna, A. Stability of gold nanostructures on rutile TiO_2(110) surface. *Surf. Sci.* **2011**, *605*, 668–674. [CrossRef]
23. Asakura, K.; Takakusagi, S.; Ariga, H.; Chun, W.J.; Suzuki, S.; Koike, Y.; Uehara, H.; Miyazaki, K.; Iwasawa, Y. Preparation and structure of a single Au atom on the TiO_2(110) surface: Control of the Au–metal oxide surface interaction. *Faraday Discuss.* **2013**, *162*, 165–177. [CrossRef] [PubMed]
24. Li, L.; Gao, Y.; Li, H.; Zhao, Y.; Pei, Y.; Chen, Z.; Zeng, X.C. CO Oxidation on TiO_2(110) Supported Subnanometer Gold Clusters: Size and Shape Effects. *J. Am. Chem. Soc.* **2013**, *135*, 19336–19346. [CrossRef] [PubMed]
25. Xu, M.; Cao, Y.; Hu, S.; Yu, M.; Wang, T.; Huang, S.; Yan, S. Manipulating the charge state of Au clusters on rutile TiO_2(110) single crystal surfaces through molecular reactions probed by infrared spectroscopy. *Phys. Chem. Chem. Phys.* **2016**, *18*, 17660–17665.
26. Kohn, W.; Sham, L.J. Quantum Density Oscillations in an Inhomogeneous Electron Gas. *Phys. Rev.* **1965**, *137*, 1697–1706. [CrossRef]
27. Kohn, W.; Sham, L.J. Self-Consistent Equations Including Exchange and Correlation Effects. *Phys. Rev.* **1965**, *140*, A1133–A1138. [CrossRef]
28. Pacchioni, G.; Giordano, L.; Baistrocchi, M. Charging of metal atoms on ultrathin MgO/Mo(100) films. *Phys. Rev. Lett.* **2005**, *94*, 226104. [CrossRef]
29. Yulikov, M.; Sterrer, M.; Heyde, M.; Rust, H.P.; Risse, T.; Freund, H.J.; Pacchioni, G.; Scagnelli, A. Binding of Single Gold Atoms on Thin MgO(001) Films. *Phys. Rev. Lett.* **2006**, *96*, 146804. [CrossRef]
30. Yulikov, M.; Sterrer, M.; Risse, T.; Freund, H.J. Gold atoms and clusters on MgO(100) films; an EPR and IRAS study. *Surf. Sci.* **2009**, *603*, 1622–1628. [CrossRef]
31. Ankudinov, A.L.; Rehr, J.J.; Low, J.J.; Bare, S.R. Sensitivity of Pt X-ray absorption near edge structure to the morphology of small Pt clusters. *J. Chem. Phys.* **2002**, *116*, 1911–1919. [CrossRef]
32. Boyanov, B.I.; Morrison, T.I. Support and Temperature Effects in Platinum Clusters. 1. Spatial Structure. *J. Phys. Chem.* **1996**, *100*, 16310–16317. [CrossRef]
33. Wang, L.L.; Khare, S.V.; Chirita, V.; Johnson, D.D.; Rockett, A.A.; Frenkel, A.I.; Mack, N.H.; Nuzzo, R.G. Origin of Bulklike Structure and Bond Length Disorder of Pt_{37} and Pt_6Ru_{31} Clusters on Carbon: Comparison of Theory and Experiment. *J. Am. Chem. Soc.* **2006**, *128*, 131–142. [CrossRef] [PubMed]
34. Costello, C.K.; Kung, M.C.; Oh, H.S.; Wang, Y.; Kung, H.H. Nature of the active site for CO oxidation on highly active Au/γ-Al_2O_3. *Appl. Catal. A* **2002**, *232*, 159–168. [CrossRef]
35. Fu, Q.; Saltsburg, H.; Flytzani-Stephanopoulos, M. Active Nonmetallic Au and Pt Species on Ceria-Based Water-Gas Shift Catalysts. *Science* **2003**, *301*, 935–938. [CrossRef]
36. Guzman, J. Structure and reactivity of a mononuclear gold complex catalyst supported on magnesium oxide. *Angew. Chem. Int. Ed. Engl.* **2003**, *42*, 690–693. [CrossRef]

37. Matsuzawa, N.; Seto, J.; Dixon, D.A. Density Functional Theory Predictions of Second-Order Hyperpolarizabilities of Metallocenes. *J. Phys. Chem. A* **1997**, *101*, 9391–9398. [CrossRef]
38. Perdew, J.P.; Chevary, J.A.; Vosko, S.H.; Jackson, K.A.; Pederson, M.R.; Singh, D.J.; Fiolhais, C. Atoms, molecules, solids, and surfaces: Applications of the generalized gradient approximation for exchange and correlation. *Phys. Rev. B* **1992**, *46*, 6671–6687. [CrossRef]
39. Perdew, J.P.; Burke, K.; Ernzerhof, M. Generalized gradient approximation made simple. *Phys. Rev. Lett.* **1996**, *77*, 3865–3868. [CrossRef]
40. Aikens, C.M. Modelling small gold and silver nanoparticles with electronic structure methods. *Mol. Simul.* **2012**, *38*, 607–614. [CrossRef]
41. Ferrando, R.; Barcaro, G.; Fortunelli, A. Structures of small Au clusters on MgO(001) studied by density-functional calculations. *Phys. Rev. B* **2011**, *83*, 045418. [CrossRef]
42. Henry, C.R. Surface studies of supported model catalysts. *Surf. Sci. Rep.* **1998**, *31*, 231–325. [CrossRef]
43. Henry, C.R. Morphology of supported nanoparticles. *Prog. Surf. Sci.* **2005**, *80*, 92–116. [CrossRef]
44. You, H.; Liu, C.J.; Ge, Q. Interaction of Pt clusters with the anatase TiO_2(101) surface: A first principles study. *J. Phys. Chem. B* **2006**, *110*, 7463–7472.
45. Gong, X.Q.; Selloni, A.; Dulub, O.; Jacobson, P.; Diebold, U. Small Au and Pt Clusters at the Anatase TiO_2(101) Surface: Behavior at Terraces, Steps, and Surface Oxygen Vacancies. *J. Am. Chem. Soc.* **2008**, *130*, 370–381. [CrossRef]
46. Zhang, J.; Zhang, M.; Han, Y.; Li, W.; Meng, X.; Zong, B. Nucleation and Growth of Palladium Clusters on Anatase TiO_2(101) Surface: A First Principle Study. *J. Phys. Chem. C* **2008**, *112*, 19506–19515. [CrossRef]
47. Pabisiak, T.; Kiejna, A. Energetics of oxygen vacancies at rutile TiO_2(110) surface. *Solid State Commun.* **2007**, *144*, 324–328. [CrossRef]
48. Kiejna, A.; Pabisiak, T.; Gao, S.W. The energetics and structure of rutile TiO_2(110). *J. Phys. Condens. Matter* **2006**, *18*, 4207. [CrossRef]